Control Strategies for DFIG based on Wind Energy Conversion System using RST and Fuzzy Logic Controllers

Bouchaib Rached
Laboratory of Signal Analysis and Information Processing
FST Settat
Morocco
bouchaib.rached@gmail.com

Mustapha Elharoussi
Laboratory of Signal Analysis and Information Processing
FST Settat
Morocco
m.elharoussi@gmail.com

Elhassane Abdelmounim
Laboratory of Signal Analysis and Information Processing
FST Settat
Morocco
hassan.abdelmounim@hotmail.fr

***Abstract*— In this paper, control strategies of the MPPT for the extraction of the maximum power for a wind energy conversion system (WECS) based on a doubly fed induction generator(DFIG) is presented.**

The main objective of this work is to compare the energy production unit performances of WECS based on DFIG connected to the electric power grid by the use of the RST and Fuzzy Logic Controllers.

In this work, an appropriate model for WECS and vector control strategy for DFIG are established. A comparative study was made between the RST and the Fuzzy Logic controller.

The performances of the proposed controllers in terms of set point tracking, speed response, and robustness with respect to sudden variations in the DFIG parameters is demonstrated through an illustrative simulation in Matlab/Simulink.

Keywords*— *WECS, MPPT, Vector Control, DFIG, Fuzzy logic controllers, RST.

I. INTRODUCTION

Wind power is increasingly becoming the first alternative renewable energy resource, this energy is greener than traditional sources such as coal or oil. It's an environmentally friendly and clean renewable energy source, also it has known an outstanding development in recent years [1][2].

The DFIG based wind energy conversion system is the most popular application among the wind-energy conversion technologies. That is due to high efficiency, energy quality and the ability to control the power supplied to the grid, small power electronic interface that carried only a third of the DFIG rated power, wider speed range of operations, which means a low mechanical stress, and a separately and easily controllable active and reactive power [3][4].

In this study, we proposed a platform for the WECS under Matlab/Simulink using two controllers independently, namely RST and Fuzzy Logic (FL). These two controllers are used to control the RSC and MPPT to achieve the following control objectives, a good static precision in order to obtain optimal energy production and robustness to any parametric variations in the DFIG.

To validate our platform, we have adopted the following test conditions: variation of the active power setpoint, the reactive power reference is maintained at zero, speed variation, and variation in rotor resistance.

The paper is organized as follows: in Section II, a description of the aerodynamic model of the wind turbine and the DFIG is presented. In Section III, a RST and fuzzy logic controllers are developed to control the rotor side converter RSC. Also, MPPT strategies based on these controls are designed. Simulation results are presented and discussed in section IV.

II. MODELING OF WECS

The WECS is mainly composed of the wind turbine, gearbox, the doubly fed induction generator whose stator is directly connected to the grid and the rotor is connected via the Rotor Side Converter (RSC) and the Grid Side Converter (GSC).

A WECS structure is shown in Figure 1:

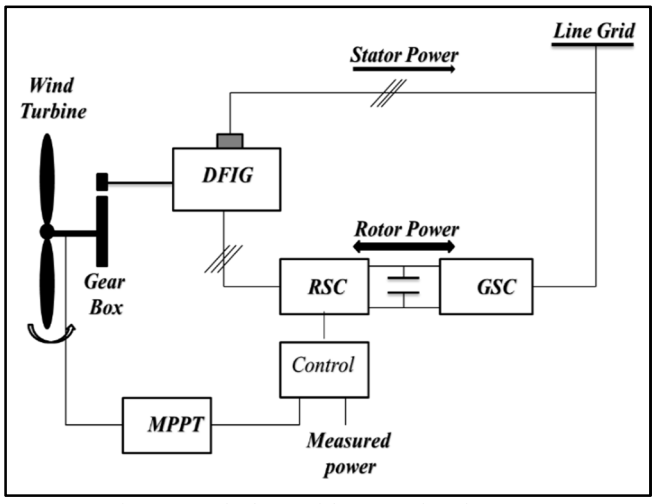

Fig.1. General scheme of the WECS based on DFIG

A. Wind turbine

The aerodynamic power captured by the wind turbine is given by [1][2]:

$$P_{aero} = \frac{1}{2} \cdot C_P(\beta,\lambda) \cdot \rho \cdot \pi \cdot R_{Pale}^2 \cdot V_{wind}^3 \qquad (1)$$

Where ρ is the air density (kg/ m³), R_{Pale} is the blade radius (m), V_{wind} is the wind speed, $C_P(\beta,\lambda)$ is the turbine power coefficient, β blade pitch angle (°), and λ is the tip speed ratio, which is defined by:

978-1-7281-0827-8/19/$31.00 ©2019 IEEE

$$\lambda = \frac{\Omega_t \cdot R_{Pale}}{V_{wind}} \tag{2}$$

Where Ω_t is the Rotational speed of the turbine.
Expression of the aerodynamic torque is given by:

$$T_{aero} = \frac{P_{aero}}{\Omega_t} = \frac{1}{2} \cdot C_P(\lambda,\beta) \cdot \rho \cdot S \cdot \frac{V_{wind}^3}{\Omega_t} \tag{3}$$

Where S is the area swept by the pales of the turbine.

The gearbox adapts the slow speed of the turbine to the speed of the generator. It is modelled by [5][6]:

$$N_G = \frac{\Omega_m}{\Omega_t} \tag{4}$$

$$T_m = \frac{T_{aero}}{N_G} \tag{5}$$

T_m is the mechanical torque on the rotor shaft of the generator.

The equation of system dynamics can be written as:

$$J \cdot \dot{\Omega}_m = T_m - K \cdot \Omega_m - T_{em} \tag{6}$$

J : the total inertia brought back to the rotor shaft of the generator;
K : Coefficient of Total Friction Returned to the Generator Rotor Shaft (Nm/rd/s).

B. DFIG model

The DFIG dynamic model is given by [7][8][9]:

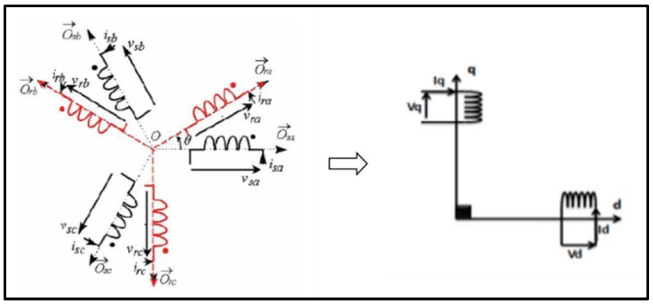

Fig. 2. DFIG model in dq frame

Electrical equations:

$$\begin{cases} V_{Sd} = R_S I_{Sd} + \dfrac{d}{dt}\Phi_{Sd} - \omega_S \Phi_{Sq} \\ V_{Sq} = R_S I_{Sq} + \dfrac{d}{dt}\Phi_{Sq} + \omega_S \Phi_{Sd} \\ V_{rd} = R_r I_{rd} + \dfrac{d}{dt}\Phi_{rd} - \omega_r \Phi_{rq} \\ V_{rq} = R_r I_{rq} + \dfrac{d}{dt}\Phi_{rq} + \omega_r \Phi_{rd} \end{cases} \tag{7}$$

Stator and rotor flux equations:

$$\begin{cases} \Phi_{Sd} = L_S I_{Sd} + M I_{rd} \\ \Phi_{Sq} = L_S I_{Sq} + M I_{rq} \\ \Phi_{rd} = L_r I_{rd} + M I_{Sd} \\ \Phi_{rq} = L_r I_{rq} + M I_{sq} \end{cases} \tag{8}$$

Stator and rotor active and reactive powers:

$$\begin{cases} P_S = v_{Sd} \cdot i_{Sd} + v_{Sq} \cdot i_{Sq} \\ Q_s = v_{Sq} \cdot i_{Sd} - v_{Sd} \cdot i_{Sq} \end{cases} \tag{9}$$

$$\begin{cases} P_r = v_{rd} \cdot i_{rd} + v_{rq} \cdot i_{rq} \\ Q_r = v_{rq} \cdot i_{rd} - v_{rd} \cdot i_{rq} \end{cases} \tag{10}$$

The electromagnetic torque :

$$T_{em} = pM\left(I_{rd} I_{Sq} - I_{rq} I_{Sd}\right) \tag{11}$$

III. CONTROL STRATEGIES OF WECS

We implement these commands strategies in order to meet the following specifications: Good static precision in order to obtain optimal energy production and a unit power factor; Robustness to any parametric variations in the system.

A. Maximum Power Point Tracking

The MPPT control is used to adjust the speed of the generator to place the operating point on the optimal power curve for each wind speed. This is one of the main advantages of variable speed wind turbines compared to those operating at fixed speed [12].

There are several maximum power point tracking techniques, among which we can cite:
•Relative speed method;
•MPPT by disruption and observation;
•Torque or power control.

In this paper, we used the torque control. In this method, in order to extract the maximum power, the specific speed must be set to its optimal value λ_{opt} in order to obtain the maximum power coefficient c_p max .

The power coefficient c_p must be maintained at its maximum value in order to reach the T_{opt} , which is given by the following equation:

$$T_{opt} = k_{opt} \cdot \Omega_m{}^2 \tag{12}$$

Where, $$K_{opt} = \frac{1}{2} \cdot \rho \cdot \pi \cdot R_{Pâle}^5 \cdot \frac{C_{PMAX}}{\lambda^3_{opt}} \tag{13}$$

a) RST Controller Synthesis for MPPT

The acronym RST comes from the name of the 3 polynomials that must be determined in order to obtain an efficient control. The polynomials R, S and T will be chosen to have the closed loop transfer function identical to a model to be continued. With this controller, there are therefore two degrees of freedom for dynamic adjustment (R(p) and S(p)).

The parameters S(p) and R(p) are calculated according to the equation [10]:

$$D = AS + BR \tag{14}$$

With: $$\deg(D(p)) = \deg(A(p)) + \deg(S(p)) \tag{15}$$

The RST controller structure is given in fig.3 [11]:

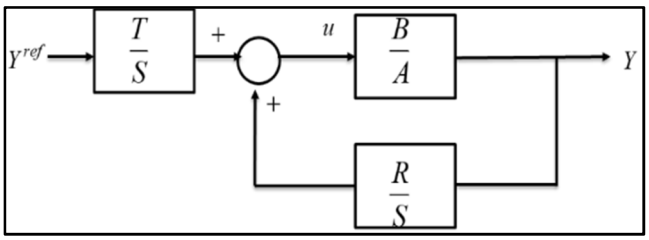

Fig.3a. RST controller structure

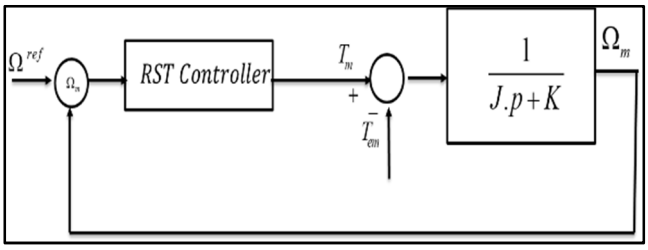

Fig.3b. RST controller for MPPT

b) Fuzzy Logic Controller Synthesis for MPPT

Fuzzy logic control (FLC) imitates human reasoning by exploiting the different information collected in linguistic form. The MPPT controller structure is represented in the figure 4 :

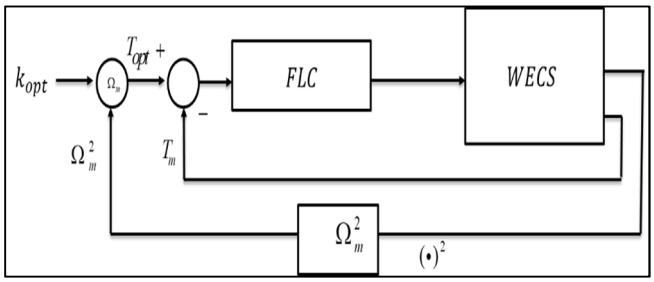

Fig.4. MPPT strategy based on FLC

The operation of the fuzzy controller is based on its capability to simulate several role implications at the same time procedure, and it results significantly comprehensive output [12][13][14].

The fuzzy control based on Mamdani model is divided into three parts as presented in figure 5 [12][13][18].

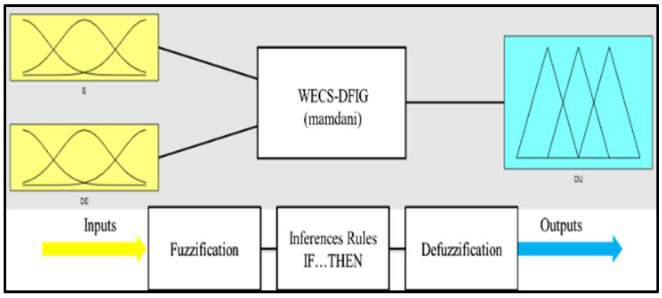

Fig.5. Block diagram of fuzzy control

Triangular and trapezoidal membership functions are used on a universe of discourse normalized in the range [-1; 1] for the inputs (error (E), error variation (DE)) and output (command) as shown in figure 6.

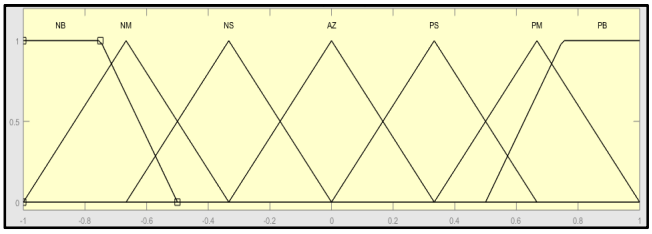

Fig.6. Membership functions

The fuzzy sets are defined as follows:

NB: Negative-Big; NM: Negative-Medium; NS: Negative-Small; AZ: About-Zero; PS: Positive-Small; NM: Positive-Medium; PB: Positive-Big.

The fuzzy rules, for determining output variable of the controller as a function of input variables are grouped in the Table 1.

Table1. Rules matrix for fuzzy logic controllers

		E						
		NB	NM	NS	AZ	PS	PM	PB
DE	NB	NB	NB	NB	NB	NM	NS	AZ
	NM	NB	NB	NB	NM	NS	AZ	PS
	NS	NB	NB	NM	NS	AZ	PS	PM
	AZ	NB	NM	NS	AZ	PS	PM	PB
	PS	NM	NS	AZ	PS	PM	PB	PB
	PM	NS	AZ	PS	PM	PB	PB	PB
	PB	AZ	PS	PM	PB	PB	PB	PB

B. Rotor Side Converter

a) Vector control of DFIG

Considering the orientation of the stator flux vector along the direct axis (FOC), the direct component of the stator voltage is zero [15][16][17]. The expressions elaborated in Eq. (8) become:

$$\phi_{Sq} = 0 \Leftrightarrow \phi_S = \phi_{Sd} \tag{16}$$

$$\begin{cases} V_{Sd} = 0 \\ V_{Sq} = \omega_S \Phi_{Sd} = V_s \end{cases} \tag{17}$$

So, we can write :

$$\begin{cases} \Phi_{Sd} = L_S I_{Sd} + M I_{rd} \\ \Phi_{Sq} = L_S I_{Sq} + M I_{rq} = 0 \end{cases} \tag{18}$$

The adaptation of the relations (9) (10), and (18) to the chosen system of axes and the simplifying hypothesis considered in our case gives:

$$\begin{cases} P_S = -V_S \dfrac{M}{L_S} I_{rq} \\ Q_S = \dfrac{V_S \Phi_S}{L_S} - \dfrac{V_S M}{L_S} I_{rd} \end{cases} \tag{19}$$

$$\begin{cases} P_r = gV_S \dfrac{M}{L_S} I_{rq} \\ Q_r = g \dfrac{V_S M}{L_S} I_{rd} \end{cases} \tag{20}$$

Therefore, power control is achieved by regulating the d and q rotor currents:

$$\begin{cases} v_{rd} = R_r I_{rd} - L_r \omega_r \sigma I_{rq} + L_r \sigma \dfrac{dI_{rd}}{dt} \\ v_{rq} = R_r I_{rq} + L_r \omega_r \sigma I_{rd} + \dfrac{M \omega_r}{L_S} \Phi_{sd} + L_r \sigma \dfrac{dI_{rq}}{dt} \end{cases} \tag{21}$$

The plant for the current control loops is given in (22) and (23):

$$F(s) = \frac{I_{rd}(s)}{V_{rd}^r(s)} = \frac{I_{rq}(s)}{V_{rq}^r(s)} = \frac{V_S M}{R_r L_s + s L_s L_r \sigma} \tag{22}$$

$$\begin{cases} e_d = g\omega_s \dfrac{M}{L_S} \phi_s \\ e_q = \dfrac{V_S R_r}{\omega_s M} \end{cases} \tag{23}$$

V_{rd}^r , V_{rq}^r and e_d , e_q are the controller output voltages and the compensation voltages respectively.

b) RST Controller Synthesis for RSC

The purpose of controlling this converter is to control the stator's active and reactive powers.

The Fig. 7 illustrates the design of this control**.**

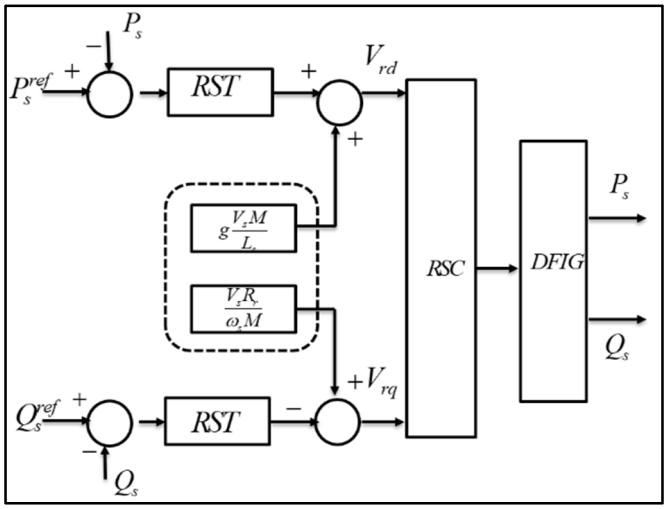

Fig. 7. Scheme of RST Controller for RSC

The proposed RST model is expressed as:

$$\begin{cases} A(p) = a_1 p + a_0 \\ B(p) = b_0 \\ D(p) = d_3 p^3 + d_2 p^2 + d_1 p + d_0 \\ R(p) = r_1 p + r_0 \\ S(p) = s_2 p^2 + s_1 p + s_0 \end{cases} \tag{24}$$

The polynomial can be written as the following:

$$D = (p + \frac{1}{T_c})(p + \frac{1}{T_f})^2 \tag{25}$$

$P_c = -\dfrac{1}{T_c}$ is the pole of polynomial C and $P_f = -\dfrac{1}{T_f}$ is the double pole of the polynomial filter F.

$$\begin{cases} P_c = 5P_a = 5\dfrac{L_s L_r}{L_s L_r - M^2} \\ T_c = \dfrac{1}{P_c} \\ T_f = \dfrac{1}{3} T_c \end{cases} \tag{26}$$

The closed-loop specifications recommend having the model to be pursued described by:

$$D = (p - 5P_a)(p - 15P_a)^2 \tag{27}$$

Through the identification of the equations (24) and (27), we can reach a system of linear equations that can be represented by the Sylvester matrix. We deduce from this the polynomials R(p), S(p), and T(p):

$$\begin{cases} d_3 = a_1 s_2 \rightarrow s_2 = \dfrac{d_3}{a_1} \\ d_2 = a_1 s_1 \rightarrow s_1 = \dfrac{d_2}{a_1} \\ d_1 = a_0 s_1 + b_0 r_1 \rightarrow r_1 = \dfrac{d_1 - a_0 s_1}{b_0} \\ d_1 = b_0 r_0 \rightarrow r_0 = \dfrac{d1}{b_0} \\ T = r_0 \end{cases} \tag{28}$$

c) Fuzzy Logic Controller Synthesis for RSC

The proposed FLC control for RSC is illustrated in Fig 8 :

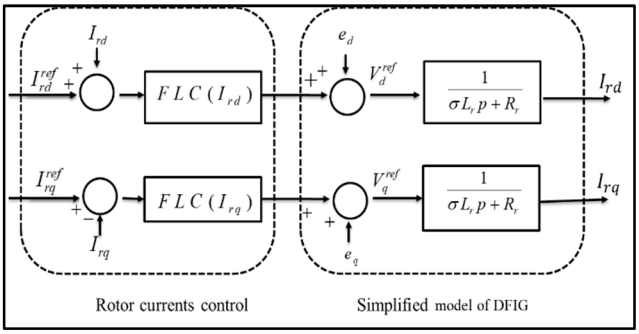

Fig.8. Schematic diagram of Fuzzy Logic Controller for RSC

Using eq.19, we can calculate the rotor current references as follows:

$$\begin{cases} I_{rq}^{ref} = -P_s^{ref} \cdot \dfrac{L_S}{\omega_s M \Phi_{sd}} \\ I_{rd}^{ref} = -Q_s^{ref} \cdot \dfrac{L_S}{MV_S} + \dfrac{\Phi_{sd}}{M} \end{cases} \tag{29}$$

$$P_s^{ref} = T_{em}^{ref} \omega_s \quad (30)$$

Where T_{em}^{ref} is the reference electromagnetic torque deduced from MPPT control strategy.

IV. CONTROLS VALIDATION AND SIMULATION RESULTS

To validate the control strategies studied in this work and compare their performances, We have adopted the following test conditions:

- Variation of the power set point. The reactive power reference is maintained at zero;
- Speed variation: at t = 10 [s], Ω :150 [rd/s] → 170 [rd/s];
- Variation in rotor resistance: t = 12 [s], Rr →2* Rr.

The parameters of WECS for a simulation are presented in table 2 [14].

The simulation results in figures (9-14) present a dynamic response of the WECS.

A. Reference tracking

The performance of the proposed controls is tested under the conditions mentioned above and the results are illustrated in the following figures.

The active and reactive powers are illustrated in figures 9 and 10.

The speed of the generator is depicted in figures 11 and 12.

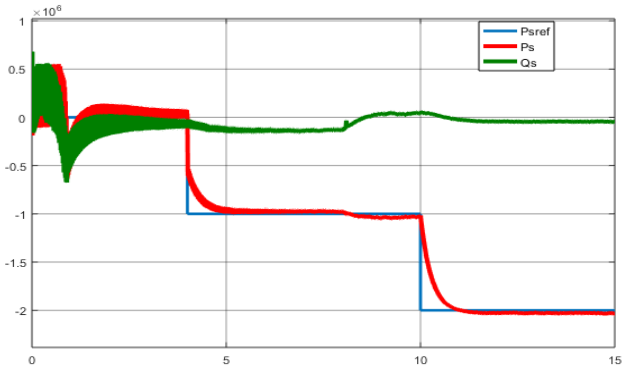

Fig.9. Stator power evolution (FLC)

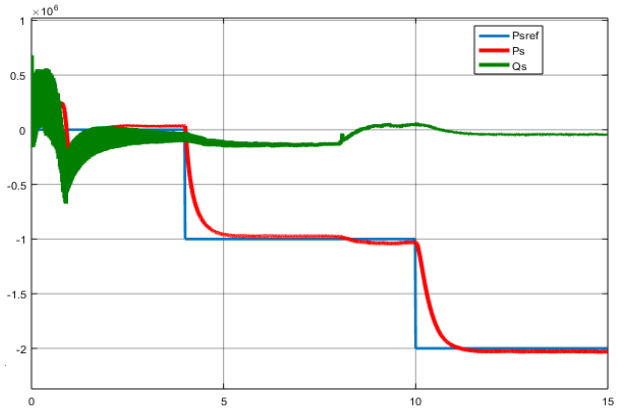

Fig.10. Stator power evolution (RST)

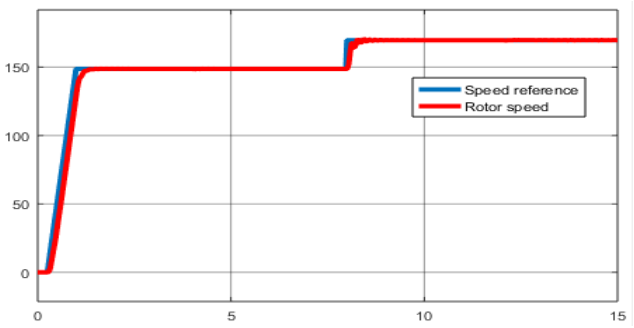

Fig. 11. Speed response (FLC)

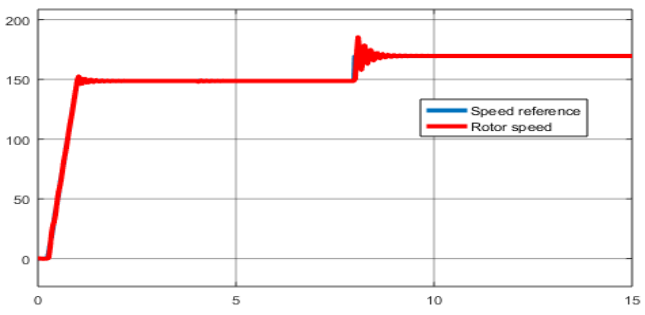

Fig. 12. Speed response (RST)

According to fig 11 and fig 12, for the mechanical speed: the response time of the RST controller is better than the fuzzy one, but at the same time, a significant overshoot is seen. In addition, for the powers (figs 9 and 10)): the fuzzy controller presents a faster response time and a faster transient response in comparison with the RST controller.

From the simulation results, the powers follow perfectly their references and with perfect decoupling between the two axes d and q at steady state.

We note that the rotor flux oriented vector control gives good performances for both RST and fuzzy logic controllers.

B. Robustness test of the proposed commands

In order to test the robustness of the proposed control strategies we have introducing a variation in the parameters of the generator, such as:

- Variation of 50% in the rotor resistance (Rr) introduced at t = 12s.

Figures 13 and 14, show the effect of this variation on the power response for RST and fuzzy logic controllers.

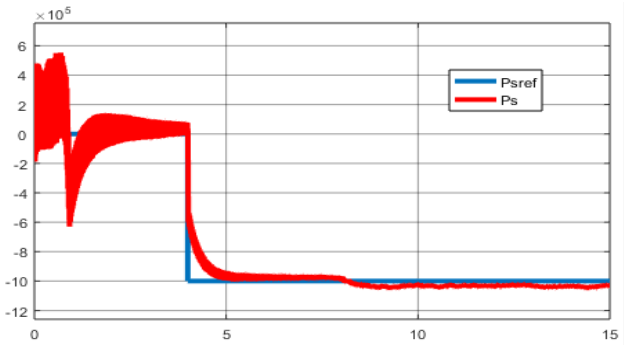

Fig.13. Evolution of stator powers during variations of Rr (FLC)

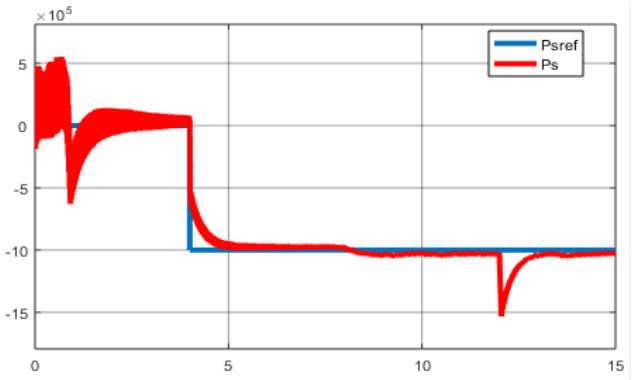

Fig.14. Evolution of stator powers during variations of Rr (RST)

From the simulation results, we note that have no influence on the performance of the FLC response. But for the RST controller, the time response is altered.

V. Conclusion

We have developed and validated a WECS platform for under Matlab/Simulink. Initially, a model for WECS is established and the vector control applied to a variable speed DFIG based wind turbine was developed. Thereafter, we have designed the RST and the fuzzy controllers, in order to meet the following specifications: performing powers reference tracking and parametric robustness. A comparative study was made between the RST and FL controllers.

The results show that the FLC presents a better performance in tracking the references compared to the RST controllers. Moreover, it provided a good dynamic behaviour of the wind system in terms of rapidity and robustness, with no overshoot and relatively simple to design since it does not require the knowledge of the exact model.

Appendix

Table2. Parameters of the DFIG

Blade Radius R	35.25 m
Rs	0.012Ω
Rr	0.021Ω
Ls	0.0137 H
Lr	0.0136 H
M	0.0135H
J	0.175 kg.m²
K	0.0024 N/rd/s
p	2
R	0.4 Ω
L	3 mH
C	2.2 mF

References

[1] I. Munteanu, Optimal control of wind energy systems : towards a global approach. Springer, 2008.

[2] G. Abad, Doubly fed induction machine : modeling and control for wind energy generation applications. Wiley-Blackwell Pub, 2011.

[3] J. A. Baroudi, V. Dinavahi, and A. M. Knight, “A review of power converter topologies for wind generators,” Renew. Energy, vol. 32, no. 14, 2007, pp. 2369–2385.

[4] V. Yaramasu and B. Wu, Model Predictive Control of Wind Energy Conversion Systems. Jhon Wiley &Sons, 2017.

[5] P. M. M. Bongers, “Modeling and Identification of Flexible Wind Turbines and A Factorizational Approach to Robust Control Design.” PhD thesis, Delft University of Technology, June 94.

[6] B. Beltran et al., “A combined high gain observer and high-order sliding mode controller for a DFIG-based wind turbine,” in Proceedings of the IEEE ENERGYCON’10, Manama (Bahraïn), December 2010, pp. 322-327.

[7] G. S. Kaloi, J. Wang, and M. H. Baloch, “Active and reactive power control of the doubly fed induction generator based on wind energy conversion system,” Energy Reports, vol. 2, Nov. 2016, pp. 194–200.

[8] C. Hamon, K. Elkington, and M. Ghandhari, “Doubly-fed induction generator modeling and control in DigSilent PowerFactory,” in 2010 International Conference on Power System Technology, 2010, pp. 1–7.

[9] A. Boyette, “Contrôle-commande d’un générateur asynchrone à double alimentation avec système de stockage pour la production éolienne,” Thèse de doctorat en génie électrique, Université Henri Poincaré, Nancy I, 11, France, 2006.

[10] W. Ouled Amor, A. Ltifi, M. Ghariani, W. O. Amor, A. Ltifi, and M. Ghariani, “Study of a Wind Energy Conversion Systems Based on Doubly-Fed Induction Generator,” Int. Rev. Model. Simulations, vol. 7, no. 4, Aug. 2014, p. 619.

[11] Z. Gadouche, C. Belfedal, T. Allaoui, and B. Belabbas, “Commande de Puissance Active et Réactive d’une MADA utilisée dans un système éolien,” 3nd Int. Semin. New Renew. Energies, no. 2, 2014.

[12] J. Trivedi and T. Agarwal, “Controlling and Analysis of Variable Wind Speed Turbine with DFIG Using Fuzzy Logic Controller,” vol. 12, no. 5, 2017, pp. 21–28.

[13] Hong Hee Lee, Phan Quoc Dzung, Le Minh Phuong, Le Dinh Khoa, and Nguyen Huu Nhan, “A new fuzzy logic approach for control system of wind turbine with Doubly Fed Induction Generator,” in International Forum on Strategic Technology 2010, 2010, pp. 134–139.

[14] B. Rached, M. Elharoussi, and E. Abdelmounim, “Fuzzy Logic Control for Wind Energy Conversion System based on DFIG,” in 2019 International Conference on Wireless Technologies, Embedded and Intelligent Systems (WITS), 2019, pp. 1–6.

[15] S. Khojet El Khil, I. Slama-Belkhodja, M. Pietrzak-David, and B. de Fornel, “Power distribution law in a Doubly Fed Induction Machine,” Math. Comput. Simul., vol. 71, no. 4–6, Jun. 2006, pp. 360–368.

[16] E. Lotfi, B. Rached, M. Elhaissouf, M. Elharoussi, and E. Abdelmounim, “DSP implementation in the loop of the vector control drive of a permanent magnet synchronous machine,” in ACM International Conference Proceeding Series, 2017, pp. 1–7.

[17] M. Elhaissouf, E. Lotfi, B. Rached, M. Elharoussi, and A. Barazzouk, “DSP Implementation in the Loop of the Indirect Rotor Field Orientation control for the Three-Phase Asynchronous Machine,” in Proceedings of the 2nd International Conference on Computing and Wireless Communication Systems - ICCWCS’17, 2017, pp. 1–7.